Int. J. Heat Mass Transfer. Vol. 16, pp. 1119–1130. Pergamon Press 1973. Printed in Great Britain

THE CALCULATION OF LOW-REYNOLDS-NUMBER PHENOMENA WITH A TWO-EQUATION MODEL OF TURBULENCE

W. P. JONES and B. E. LAUNDER

Department of Mechanical Engineering, Imperial College, Exhibition Road, London S.W.7, England

(*Received* 16 *February* 1972 *and in revised form* 18 *September* 1972)

Abstract—The paper presents numerical predictions of various turbulent shear flows in which the structure of the viscous sublayer exerts appreciable influence on the flow. The model of turbulence employed is one where the turbulence energy and its dissipation rate are calculated by way of transport equations which are solved simultaneously with the conservation equations for the mean flow.

The flows considered include isothermal low Reynolds number pipe flows, and wall boundary layers with streamwise pressure gradient and wall injection; the predictions span both natural transition and laminarisation. Although complete agreement with experiment is not yet achieved in every case, it is argued that only a turbulence model of (at least) this level of complexity will permit a universal modelling of the near-wall turbulence structures commonly found in thermal power equipment.

NOMENCLATURE

c_1, c_2, c_μ,	constants or functions of turbulence Reynolds number appearing in turbulence model;
c_f,	skin friction coefficient;
H,	shape factor (displacement thickness/momentum thickness);
k,	turbulence kinetic energy;
K,	acceleration parameter;
M,	(wall suction velocity)/u_G;
R,	radius of pipe;
Re,	pipe flow Reynolds number based on bulk velocity and pipe diameter;
R_T,	turbulence Reynolds number;
u, v, w,	mean velocity in x, y, z directions;
u', v', w',	fluctuating components of velocity in x, y, z directions;
x, y, z,	cartesian coordinates denoting streamwise, cross-stream and lateral directions respectively;
ε,	kinematic energy dissipation rate;
λ,	thermal conductivity/specific heat at constant pressure;
μ,	dynamic viscosity;
ν,	kinematic viscosity;
ρ,	density;
σ,	molecular Prandtl number;
σ_ϕ,	turbulent Prandtl number (ϕ may stand for k, ε, h);
τ,	shear stress.

Subscripts

G,	denotes free-stream value;
k, ε, h,	pertaining of diffusional transport of turbulence energy, dissipation rate or enthalpy respectively;
T,	denotes equivalent turbulent value;
overbars,	signify space or time averages as appropriate.

1. INTRODUCTION

ONE OF the most important and least understood aspects of turbulence is that which occurs when the local Reynolds number of the turbulence is low. For the effective design of many thermal process components depends crucially on recognising and accounting for the role of the turbulent motions immediately adjacent to a wall. The presence of the wall ensures that over a finite region of the flow, however thin, the turbulence Reynolds number is low enough for molecular viscosity to influence directly the processes of production, destruction and transport of turbulence. And these viscous interactions in turn render the problem of creating a general mathematical model of the turbulence at least an order of magnitude more difficult than for high-Reynolds-number flows.

Notwithstanding the above remarks, it is possible, under favourable circumstances, to escape the inherent complexities of low-Reynolds-number turbulence. For if gradients in static pressure parallel to the surface are small and if mass injection through the wall and property gradients in the fluid are, likewise, small or absent, both mean and turbulence quantities are nearly-universal functions of the normal-distance Reynolds number, y^+. Thus, the near-wall effective viscosity distribution deduced from experimental data of one flow may be employed to calculate mean velocity profiles in many others. Patankar and Spalding [1] were among the first to exploit this comparative universality of the near wall region. They used a version of Van Driest's [2] formula for the variation of mixing length near the wall to obtain satisfactory predictions of a variety of boundary layer flows.

Not all boundary layers, however, possess a turbulence structure near the wall which conforms with this "universal" pattern. It has been well established that severe streamwise pressure gradients and surface mass fluxes may substantially disturb the near wall flow [3–5], as may likewise steep property gradients or the influences of buoyancy, centrifugal or Coriolis forces [6–8]. A number of workers, including the present authors, have attempted to account for the effects of the first two of the above parameters within the framework of the Prandtl mixing-length hypothesis. Often [9–12] the mixing-length distribution is chosen to be a function of dimensionless pressure-gradient and/or mass-transfer parameters; and in this way one may certainly improve upon the accuracy of prediction generated by Van Driest's original proposal.

We have nevertheless now abandoned the above approach, for we came to believe that completely successful prediction of non-equilibrium processes in the low-Reynolds-number flow could *not* be achieved with a transport hypothesis based so firmly on local equilibrium notions. If the length scale of turbulence near the wall is not the same in a strongly accelerated flow as in a zero-pressure-gradient boundary layer then it is because the turbulence generation and decay rates are affected by convective and diffusive transport processes; and these are not the same in the two flows. Thus one ought really to determine the length scale from a transport equation either for the length scale itself or for some other equivalent variable.

In fact the use of turbulence models in which one or more turbulence quantities are found from the solution of approximated transport equations is now becoming quite commonplace. Launder and Spalding [13] have made a survey of recent proposals and have argued that models of the two-equation kind are especially to be recommended for boundary-layer flow. The solution of these equations provides the length and time scales, l and t, of the active part of the turbulent motion; the turbulent stress is then obtained by multiplying the local mean rate of strain by the turbulent viscosity of the fluid, μ_T, where

$$\mu_T \equiv c'_\mu \rho l^2/t \qquad (1.1)$$

and, at high Reynolds numbers, c'_μ is a constant. There are a number of variants of equation (1.1). The turbulence kinetic energy equation is, without exception, one of those employed in two-equation turbulence models. Thus equation (1.1) is more usually written as

$$\mu_T \equiv c''_\mu \rho k^{\frac{1}{2}} l, \qquad (1.2)$$

k denoting the turbulence energy. Moreover, it turns out that the length scale itself is not a particularly well-conditioned variable to employ as the dependent variable of the second equation. Instead workers have selected variables of the form $k^a l^b$ where a and b are constants. For example Ng and Spalding [14] and Rodi and Spalding [15] have chosen the product kl while Harlow and Nakayama [16] proposed an equation for the turbulence energy dissipation rate, ε, which may be interpreted as proportional to $k^{\frac{3}{2}}/l$. With the latter variable, equation (1.2) may be recast

$$\mu_T \equiv c_\mu \rho k^2/\varepsilon. \tag{1.3}$$

It is the last of the above forms that will be employed here.

In a recent paper [17] the authors have proposed a two-equation model which they applied to the prediction of convective heat transfer processes in strongly accelerated boundary layers. The outcome was encouraging for the predictions faithfully reproduced the measured depressions in Stanton number in regions of high acceleration. Here we report the outcome of extending the application of the model to flows with mass transfer and to flow in pipes at low Reynolds number and at high Prandtl number. The model, together with some explanation for the form chosen, is given in section 2. Section 3 presents the outcome of the predictions and discusses the relative successes and shortcomings of the model in its present form; finally in section 4 we mention further extensions and refinements of the model.

2. THE MODEL OF TURBULENCE

The hydrodynamic predictions presented in section 3 have been obtained from the solution of the following system of differential and auxiliary equations:

Streamwise momentum

$$\rho u \frac{\partial u}{\partial x} + \rho v \frac{\partial u}{\partial y} = \frac{\partial}{\partial y}\left(\mu \frac{\partial u}{\partial y} - \rho \overline{u'v'}\right) - \frac{\mathrm{d}p}{\mathrm{d}x} \tag{2.1}$$

Turbulent viscosity hypothesis

$$-\rho \overline{u'v'} = \mu_T \frac{\partial u}{\partial y} \equiv (c_\mu \rho k^2/\varepsilon)\frac{\partial u}{\partial y} \tag{2.2}$$

Turbulence kinetic energy

$$\rho u \frac{\partial k}{\partial x} + \rho v \frac{\partial k}{\partial y} = \frac{\partial}{\partial y}\left[\left(\mu + \frac{\mu_T}{\sigma_k}\right)\frac{\partial k}{\partial y}\right] + \mu_T\left(\frac{\partial u}{\partial y}\right)^2 - \rho\varepsilon - 2\mu\left(\frac{\partial k^{\frac{1}{2}}}{\partial y}\right)^2 \tag{2.3}$$

Turbulence "dissipation" rate

$$\rho u \frac{\partial \varepsilon}{\partial x} + \rho v \frac{\partial \varepsilon}{\partial y} = \frac{\partial}{\partial y}\left[\left(\mu + \frac{\mu_T}{\sigma_\varepsilon}\right)\frac{\partial \varepsilon}{\partial y}\right] + c_1 \frac{\varepsilon}{k}\mu_T\left(\frac{\partial u}{\partial y}\right)^2 - \frac{c_2 \rho \varepsilon^2}{k} + 2{\cdot}0\frac{\mu\mu_T}{\rho}\left(\frac{\partial^2 u}{\partial y^2}\right)^2. \tag{2.4}$$

In the above set, equations (2.1) and (2.2) are well known and, with the exception of the last term appearing in it, so is the simulated form of the turbulence energy equation, equation (2.3). The reasons for including this extra term are computational rather than physical; for, in solving the ε equation, there are decisive advantages, in letting ε go to zero at the wall. However, the turbulence dissipation rate is *not* zero there; it is in fact equal to

$$\mu\left[\overline{\left(\frac{\partial u'}{\partial y}\right)^2} + \overline{\left(\frac{\partial w'}{\partial y}\right)^2}\right].$$

So, we have introduced the extra term in equation (2.3) which is equal to the dissipation rate in the immediate vicinity of the surface (see [17]) and which is negligible in regions where the Reynolds number is high.

There is perhaps less familiarity with the equation for ε than with that for turbulence energy. An exact equation for this quantity may readily be derived from the Navier–Stokes equations [16] but then the unknown turbulence

c

correlations in that equation must be approximated in terms of known or calculable quantities. It is the approximated form which appears as equation (2.4). In form it parallels very closely the k-equation: each equation adopts the assumption that diffusional transport proceeds at a rate proportional to the product of the turbulent viscosity and the gradient of the property in question (the terms σ_k and σ_ε thus have the significance of turbulent Prandtl numbers). Moreover the principal generation and decay terms (the former arising through mean velocity gradients) in the two equations are likewise similar. The last term in the equation is one that we found necessary to include in order that the distribution of kinetic energy within the viscosity-affected region should be in reasonable accord with experiment. Its presence is one of the less satisfactory features of the present model and it is likely that future research will lead to its replacement by something better.

To complete the specification of the model the quantities c_μ, c_1, c_2, σ_k and σ_ε must be prescribed. At high Reynolds numbers these are all supposed to take on the constant values given in Table 1. Hanjalic and Launder [27] have discussed in some detail the basis for choosing these constants. Here therefore it may suffice to remark that: c_μ is fixed by the requirement that in a constant-stress layer $\tau_w/\rho k = c_\mu^{\frac{1}{2}}$; c_2 is determined by reference to the decay of grid turbulence; and c_1 is chosen so that the von Kármán constant equals 0·42. The diffusion coefficients σ_k and σ_ε were fixed in [17] by computer optimisation.

Table 1. High Reynolds number values of empirical constants

c_μ	c_1	c_2	σ_k	σ_ε
0·09	1·45	2·0	1·0	1·3

At low Reynolds numbers two of these, c_μ and c_2, become dependent upon the value of the turbulence Reynolds number, R_T, which we now quantify as the parameter $(\rho k^2/\varepsilon\mu)$. The functional dependences chosen are:

$$c_\mu = 0{\cdot}09 \exp(-2{\cdot}5/(1 + R_T/50)) \tag{2.5}$$

$$c_2 = 2{\cdot}0(1{\cdot}0 - 0{\cdot}3 \exp(-R_T^2)). \tag{2.6}$$

The parabolic partial differential equations (2.1), (2.3) and (2.4) (or their equivalents for axisymmetric pipe flows) have been solved by means of an adapted version of the Patankar–Spalding [1] finite-difference procedure in which 97 cross-stream intervals were employed, approximately half of which were concentrated in the 10 per cent of the boundary layer closest to the wall. At the wall both k and ε were set to zero. In cases where the outer boundary of the flow was an irrotational fluid stream, the values of k and ε there were determined from the degenerate forms of (2.3) and (2.4) which result when gradients with respect to y are set to zero. For pipe flow calculations, the gradients of k and ε were set to zero at the axis.

Provided the density is uniform, the above paragraphs provide a complete specification of the hydrodynamic field. When, however, the thermal field is of interest, the enthalpy conservation equation must also be solved. For fluids of uniform specific heat, the two-dimensional boundary-layer form of the equation may be written:

$$\rho u \frac{\partial T}{\partial x} + \rho v \frac{\partial T}{\partial y} = \frac{\partial}{\partial y}\left(\lambda \frac{\partial T}{\partial y} - \rho \overline{v'T}\right) \tag{2.7}$$

where λ denotes the thermal conductivity divided by the specific heat at constant pressure. In consonance with equation (2.2), the turbulence correlation appearing in equation (2.7) is approximated as follows:

$$-\rho \overline{v'T} = \lambda_T \frac{\partial T}{\partial y} \equiv \frac{\mu_T}{\sigma_h} \frac{\partial T}{\mathrm{d}y}. \tag{2.8}$$

The term σ_h, which is the turbulent Prandtl number for enthalpy transport, is assigned the value 0·9, independent of Reynolds numbers, for all the heat-transfer calculations presented below.

3. COMPARISON OF PREDICTIONS WITH EXPERIMENT

Comparison is made first with Laufer's [18] data of fully-developed flow in a pipe at a Reynolds number, based on maximum velocity and pipe diameter, of 5×10^5. Here the Reynolds number is so high that the viscosity-dependent region occupies barely 1 per cent of the width of the flow and the (total) shear stress within this region is sensibly uniform. These data are thus often regarded as providing a standard against which departures from normalcy in other low Reynolds number flows may be judged.

It is seen from Fig. 1 that over the bulk of the flow and within the near-wall region the calculated mean velocity profile is in reasonably good agreement with the measurements. One flaw in the model, which will display its effect later as well, is that for values of y^+ between about 15 and 30 the predicted turbulent viscosity is somewhat too high and consequently the predicted velocity at $y^+ = 34$ is a little too low. The general appearance of the kinetic energy predictions is again in general accord with the data, the agreement being particularly close for values of y^+ below 18. The measured energy peak is about 12 per cent higher than the predicted and occurs further from the wall: however, considering the uncertainties in the measurement of turbulence energy, this measure of agreement is probably satisfactory.

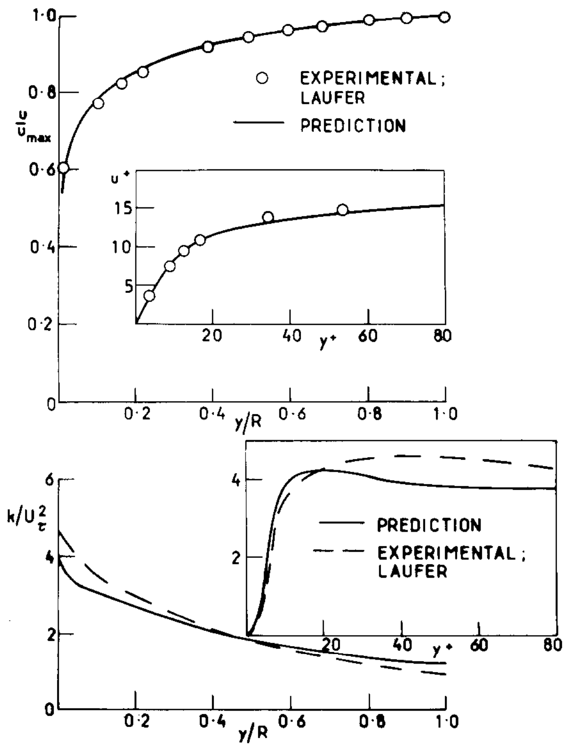

FIG. 1. Profiles in high *Re* pipe flow.

For the above case, no particular credit can be claimed for the turbulence model* since the form of the viscosity-dependent terms appearing in it was largely *determined* by reference to these data and the very similar work of Klebanoff [19]. We turn now, however, to the self-preserving flow which arises between converging plane walls, usually referred to as a sink flow. Here, the local Reynolds number, shape factor and friction coefficient of the boundary layer are constant from station to station, their values depending on the prevailing level of acceleration which is conveniently represented by the parameter

$$K \equiv \frac{\nu}{u_G^2}\frac{du_G}{dx}.$$

When the acceleration is large ($K > 10^{-6}$) the low Reynolds number structure of this flow by no means conforms with Laufer's data: the turbulent viscosity near the wall is diminished and consequently the viscous region is appreciably thicker than in high-Reynolds-number pipe flow. The effect is apparent in Fig. 2 which compares the predicted values of the shape factor, H, with measurements at various levels of

* It is perhaps worth underlining the question of universality, however. Precisely the same model has been employed here as was used in [17] to predict Klebanoff's data of boundary layer in zero pressure gradient [19]. With the mixing-length model, however, the mixing length needs to be ascribed substantially different values in the outer regions of the two flows. It might also be remarked that the *same* two-equation model leads to good predictions of many free shear flows as well.

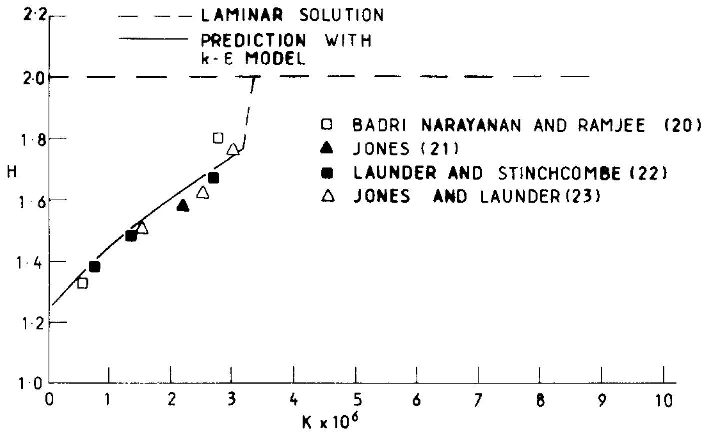

FIG. 2. Sink flow turbulent boundary layers.

acceleration. The data show a progressive rise in the value of H towards that of the laminar sink-flow boundary layer as K is increased; this behaviour is mainly a consequence of the thickening of the viscous sublayer. The predictions reasonably reproduce this measured variation. Moreover, for values of K greater than about $3{\cdot}2 \times 10^{-6}$ it turns out that the only solution to the set of equations presented in section 2 is the *laminar* one. That is, if one starts off the calculations in, say, zero pressure gradient, to let the turbulent boundary layer become well established, and then imposes a constant-K acceleration, the turbulence will

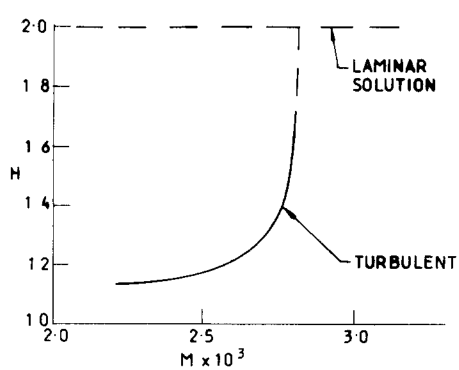

FIG. 3. Asymptotic suction boundary layers.

undergo progressive and complete decay to a laminar flow. Experimental research has not yet succeeded in delineating precisely at what value of K degeneration to laminar flow does in fact ensue; but it is certainly close to the predicted value.

Predictions of a class of flow which is closely related to the sink flow are shown in Fig. 3. They relate to asymptotic suction boundary layers and the level of the shape factor is shown as a function of the wall-suction parameter, M. Only predictions are shown because we did not regard any of the available data of sucked boundary layers as being sufficiently close to the asymptotic state to make quantitative comparison worthwhile. Here the main interest turns on the great sensitivity of the sublayer structure to the level of suction. For $M = 2{\cdot}6 \times 10^{-3}$ the shape factor is 1·2, a value typical of high-Reynolds-number flow yet at $M = 2{\cdot}8 \times 10^{-3}$ the boundary layer is on the verge of decay to laminar. The results are consistent with the data of Simpson *et al.* [5] for $M = 0{\cdot}003$ which seem to show the boundary layer is decaying to laminar.

We now return to the case of fully-developed pipe flow, only this time for low Reynolds numbers. In Fig. 4a comparison is drawn

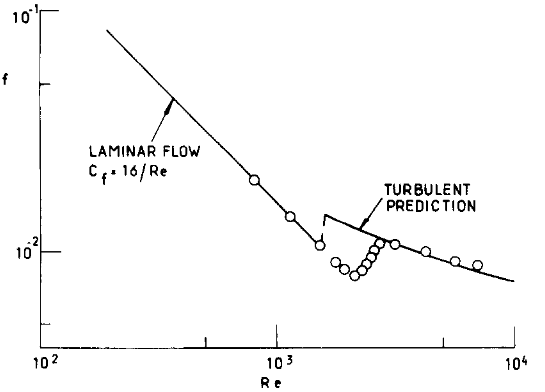

FIG. 4a. Low-*Re* pipe flow.

between the friction factor measurements of Patel and Head [24] and those predicted by our turbulence model. For Reynolds numbers greater than 3×10^3 the predicted values are within 2 per cent of the measured. However, while the measurements exhibit a shift from turbulent to laminar flow over the range of Reynolds numbers from $2{\cdot}8 \times 10^3$ to $2{\cdot}0 \times 10^3$, the predicted flow remains turbulent down to a Reynolds number of $1{\cdot}6 \times 10^3$, whereupon, if *Re* is further reduced, the flow promptly reverts to laminar. The equivalent comparisons for the

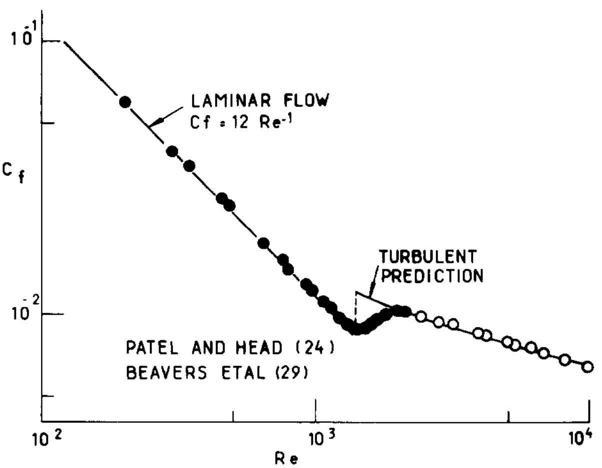

FIG. 4b. Low-*Re* channel flow.

case of flow through a plane channel are provided in Fig. 4b. Here the experimental data are those of Patel and Head [24] for $Re \leqslant 2 \times 10^3$ and those of Beavers *et al.* [29] for $Re \geqslant 2{\cdot}5 \times 10^3$.* Again, excellent agreement between experiment and prediction is obtained in the fully turbulent regime but the calculated transition back to laminar flow occurs at too low a Reynolds number and too abruptly.

We believe (as other workers have suggested) that the measured decrease in c_f as the Reynolds number is lowered is associated with the flow being *intermittently* laminar and turbulent; it thus seems to us unlikely that the phenomenon will be adequately predicted with a steady state analysis such as we have made.

An interesting feature of the pipe-flow predictions emerges in Fig. 5 where velocity profiles in $u^+ \backsim y^+$ co-ordinates are plotted. Figure 5a, which shows predicted profiles at three Reynolds numbers, indicates that there is no truly "universal" region. Even for a Reynolds number as high as 25 000, viscous influences cause the effective slope of the semi-logarithmic region of the velocity profile to be distinctly higher than at very large Reynolds numbers.† This trend is certainly in agreement with the available experimental data. For example, the velocity profile of Kudva and Sesonske [28] at a Reynolds number of 6000 shown in Fig. 5b strongly supports the present predictions. These results certainly go some way towards explaining the very different values proposed by different workers for the two experimentally determined constants in the semi-logarithmic law. Moreover, they show why friction-factor formulae based on

* The data of [24] obey the relation $c_f = 0{\cdot}0376\ Re^{-\frac{1}{6}}$ for $Re > 2 \times 10^3$. This result is substantially at variance with the extensive data of Beavers *et al.* Since these latter measurements were extensive and obtained in several different configurations it seems likely that the data of Patel and Head are in error.

† In this class of flow convective transport is zero. The behaviour of the predictions is thus solely attributable to diffusive processes.

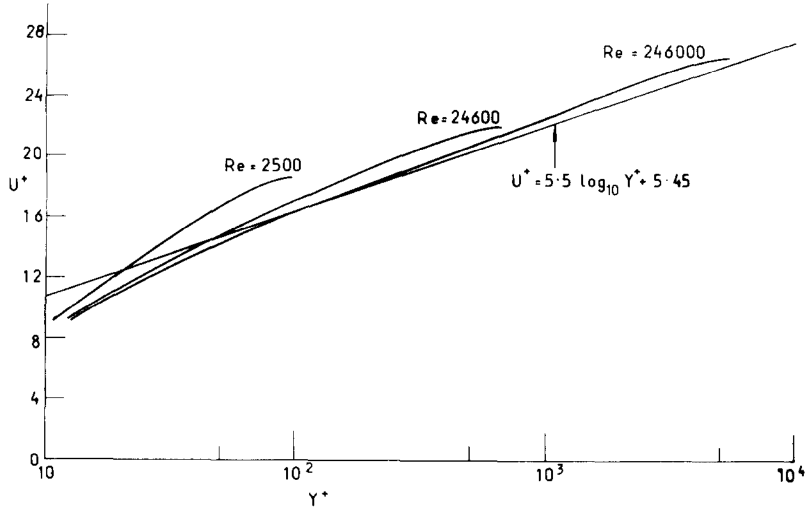

FIG. 5a. Dependence of $u^+ \sim y^+$ profiles on Re.

the notion of a "universal" velocity profile give too high values of friction factor at low Reynolds numbers.

The remaining predictions are concerned with heat transfer. Figure 6 compares the Stanton number in fully-developed pipe flow with the experimental data collected by Deissler [25]. It is seen that agreement is generally satisfactory though at very high Prandtl numbers the predicted Stanton number is somewhat too high.

The result provides support for our suggestion that the model generates turbulent viscosities which are rather too high in the vicinity of the

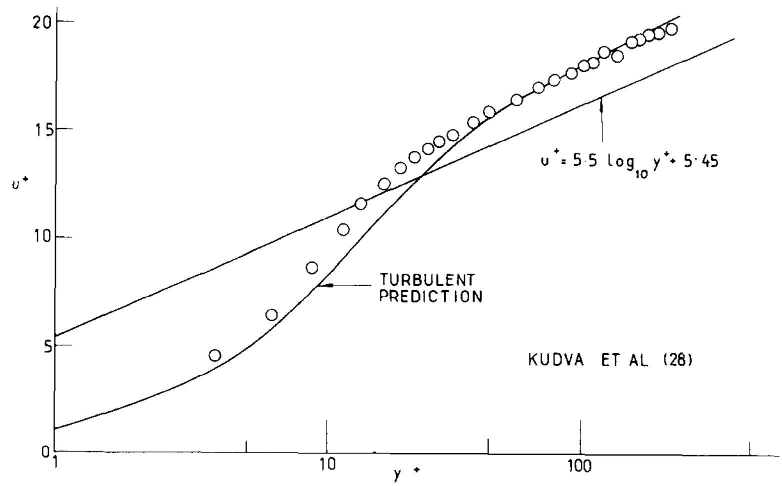

FIG. 5b. Pipe-flow velocity profile: $Re = 6000$.

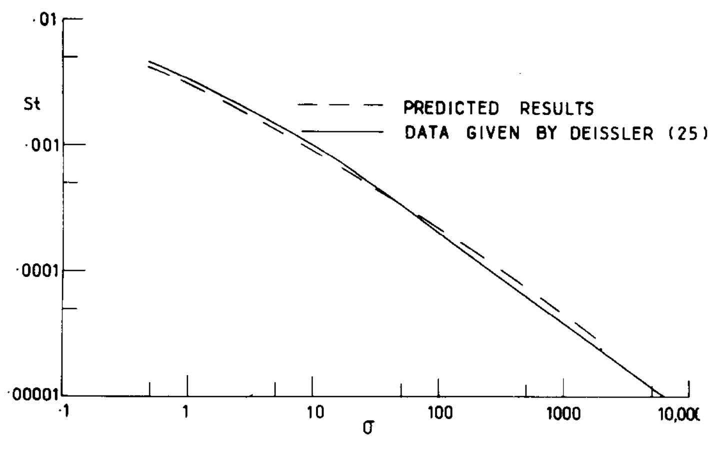

FIG. 6. Heat transfer at high Prandtl number.

wall (for, as σ is progressively increased, the turbulence structure immediately adjacent to the wall becomes increasingly dominant in determining the level of Stanton number).

All the flows considered so far have been self preserving ones. For the final comparisons, therefore, we turn to two flows where abrupt changes occur in the streamwise direction. The data are some of those obtained by Kearney *et al.* [26] involving step changes in the level of surface blowing rates and in streamwise pressure gradient. The measured and predicted distributions of Stanton number along the plate are shown in Figs. 7 and 8. The general accord between experiment and prediction is quite good, although some detailed discrepancies remain. It is not yet clear to us whether, in Fig. 7, the large difference between the measured and predicted Stanton number at $x = 3{\cdot}2$ ft is a shortcoming of the measurements or the predictions. In Fig. 8, however, we are sure that the model is at fault in predicting too slow an increase in Stanton number downstream from the end of the acceleration (the same discrepancy has been found in [17] for flows without mass transfer).

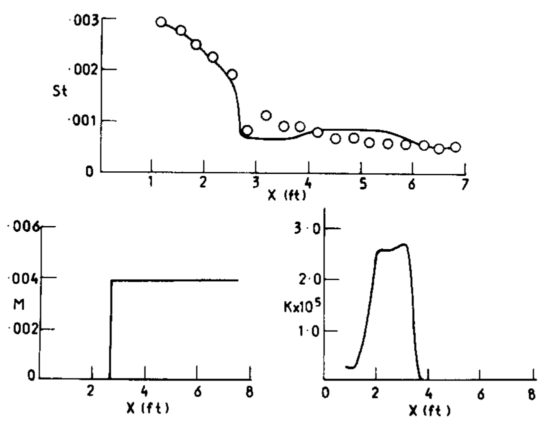

FIG. 7. Heat transfer with blowing and acceleration, Kearney *et al.* run 102469-1.

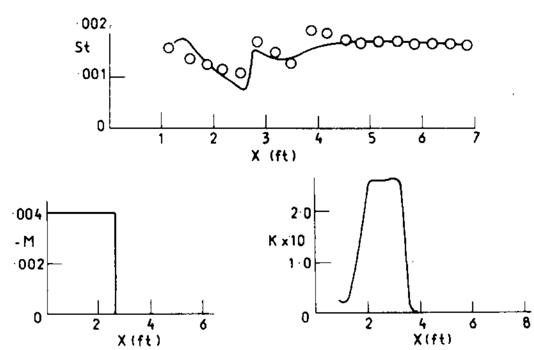

FIG. 8. Heat transfer with blowing and acceleration, Kearney *et al.* run 11369-2.

4. CONCLUDING REMARKS

The foregoing section has presented predictions of a number of wall boundary layers for cases where the region of low turbulence Reynolds numbers differs from that found in high-Reynolds-number pipe flows. Generally the two-equation model of turbulence employed has acquitted itself well, particularly considering that the disposable functions of turbulence Reynolds number appearing in it were chosen to secure agreement with standard high-Reynolds-number flows. The prediction scheme thus has some claim to be regarded as fundamental.

Of course, agreement with experimental data is yet by no means perfect and perhaps some of the recent mixing-length proposals yield nearly as good results. But mixing-length models make rather direct appeal to experimental data. Moreover, in many of the interesting low-Reynolds-number turbulence phenomena we must account for free-stream turbulence and significant body-force terms, besides those parameters considered here. It does not look fruitful to us to attempt to encompass all these effects within the framework of the mixing-length hypothesis.

Finally it is appropriate to mention extensions and improvements of the model. We have already mentioned that the c_μ function needs adjustment and there are probably similar refinements that can be performed on the other viscosity dependent terms. A further and more radical refinement would be the provision of a transport equation for the turbulent shear stress; this would replace the present turbulent viscosity formula, equation (2.2), in the mean momentum equation. The equation would contain k and ε as unknowns so the transport equations for these variables would also need to be retained. A model of this kind has already been tested [27] but it is applicable only to regions where the turbulence is not directly affected by viscosity. Its extension to regions of low Reynolds number would seem profitable. It is our impression that such a model would provide more reliable predictions than the present one of transition phenomena in turbulence especially in flows where the structure undergoes rapid changes in the streamwise direction.

ACKNOWLEDGEMENTS

We gratefully acknowledge the support provided by the Science Research Council through contract B/SR/5049.

REFERENCES

1. S. V. PATANKAR and D. B. SPALDING, *Heat and Mass Transfer in Boundary Layers*. Morgan Grampian, London (1967).
2. E. R. VAN DRIEST. On turbulent flow near a wall, *J. Aero Sci.* **23** (1956).
3. B. E. LAUNDER, Laminarization of the turbulent boundary layer by acceleration, M.I.T. Gas Turbine Lab Rep 77 (1964).
4. P. M. MORETTI and W. M. KAYS, Heat transfer to a turbulent boundary layer with varying surface temperature– an experimental study, *Int. J. Heat Mass Transfer* **8** (1965).
5. R. L. SIMPSON, R. J. MOFFAT and W. M. KAYS, The turbulent boundary layer on a porous plate: An experimental study of the fluid dynamics with suction and injection, Univ. Stanford Thermosciences Div. Rep HMT-2 (December 1967).
6. H. C. PERKINS and P. M. WORSØE-SCHMIDT, Turbulent heat and momentum transfer for gases in a circular tube at wall-to-bulk temperature ratios of seven, *Int. J. Heat Mass Transfer* **8** (1965).
7. W. B. HALL and J. D. JACKSON, Laminarisation of a turbulent pipe flow by buoyancy forces, ASME paper 69-HT-55 (1969).
8. J. P. JOHNSTON, The suppression of shear layer turbulence in rotating systems, AGARD Conference on Turbulent Shear Flows Preprint 93, London (1971).
9. W. P. JONES and B. E. LAUNDER, On the prediction of Laminarescent turbulent boundary layers, ASME paper 69-HT-13 (1969).
10. W. M. KAYS, R. J. MOFFAT and THIELBAHR, Heat transfer to the highly accelerated turbulent boundary layer with and without mass addition, *J. Heat Transfer* (1970).
11. T. CEBECI and G. J. MOSINSKIS, Predictions of turbulent boundary layers with mass addition including highly accelerating flows, *J. Heat Transfer* (1970).
12. T. E. POWELL and A. B. STRONG, Calculations of the 2-dimensional turbulent boundary layer with mass addition and heat transfer, Proc. Heat Transfer and Fluid Mech Inst. Stanford University (1970).
13. B. E. LAUNDER and D. B. SPALDING, Turbulence Models and their application to the prediction of Internal Flows, Symposium on Internal Flows, Inst. of Mech. Engns (1971).
14. K. H. NG and D. B. SPALDING, Some applications of a

model of turbulence for boundary layers near walls, *Physics Fluids* **15** (1972).
15. W. RODI and D. B. SPALDING, A two-parameter model of turbulence and its application to free jets, *Wärme und Stoffübertragung* **3** (1970).
16. F. H. HARLOW and P. I. NAKAYAMA, Transport of turbulence energy decay rate, Los Alamos Sci Lab Rep LA-3854 (1968).
17. W. P. JONES and B. E. LAUNDER, The prediction of laminarization with a 2-equation model of turbulence, *Int. J. Heat Mass Transfer* **15**, 301 (1972).
18. J. LAUFER, The structure of turbulence in fully developed pipe flow, NACA Rep 1174 (1953).
19. P. S. KLEBANOFF, Characteristics of turbulence in a boundary layer with zero pressure gradient NACA Rep 1247 (1955).
20. M. A. BADRINARAYANAN and V. RAMJEE, On the criteria for reverse transition in a two-dimensional boundary layer flow *J. Fluid Mech.* **31** (1968).
21. W. P. JONES, Strongly accelerated turbulent boundary layers, M.Sc. Thesis, University of London (1967).
22. B. E. LAUNDER and H. S. STINCHCOMBE, Non-normal similar turbulent boundary layers, Imperial College Mech Eng Dept Rep TWF/TN/21 (1967).
23. W. P. JONES and B. E. LAUNDER, Some properties of sink-flow boundary layers, *J. Fluid Mech.* **56**, 337 (1972).
24. V. C. PATEL and M. R. HEAD, Some observations on skin friction and velocity profiles in fully developed pipe and channel flows, *J. Fluid Mech.* **38**, 181 (1969).
25. R. G. DEISSLER, Analysis of Turbulent heat transfer and friction in smooth pipes at high Prandtl or Schmidt numbers, NACA Rep 1210 (1955).
26. D. W. KEARNEY, R. J. MOFFAT and W. M. KAYS, The turbulent boundary layer: experimental heat transfer with strong favourable pressure gradients and blowing, Univ. Stanford, Thermosciences Div Rep HMT-12 (1970).
27. K. HANJALIC and B. E. LAUNDER, A Reynolds stress model of turbulence and its application to thin shear flows, *J. Fluid Mech.* **52**, 609 (1972).
28. A. K. KUDVA and A. SESONSKE, Structure of turbulent velocity and temperature fields in ethylene glycol pipe flow at low Reynolds number, *Int. J. Heat Mass Transfer* **15**, 127 (1972).
29. G. S. BEAVERS, E. M. SPARROW and J. R. LLOYD, Low Reynolds number turbulent flow in large aspect ratio rectangular ducts, *J. Basic Engng* **93**, 296 (1971).

LE CALCUL DES PHENOMENES A BAS NOMBRE DE REYNOLDS A L'AIDE D'UN MODELE A DEUX EQUATIONS DE TURBULENCE

Résumé—L'article présente des estimations numériques de divers écoulements turbulents dans lesquels la structure de la sous-couche visqueuse exerce une influence notable sur l'écoulement. On a employé un modèle de turbulence où l'énergie de turbulence et son taux de dissipation sont calculés à l'aide des équations de transport résolues simultanément avec les équations de conservation pour l'écoulement moyen.

Les écoulements considérés comprennent les écoulements isothermes en conduite à faibles nombres de Reynolds, les couches limites de paroi avec un gradient de pression dans le sens de l'écoulement et l'injection à la paroi. Les estimations concernent à la fois la transition naturelle et la laminarisation. Bien qu'un accord complet avec l'expérience ne soit pas encore obtenu on prouve qu'un tel modèle de turbulence avec ce niveau minimal de complexité permettra seulement une modélisation universelle des structures de turbulence près de la paroi communément réalisées dans les équipements thermiques.

DIE BERECHNUNG VON STRÖMUNGEN NIEDRIGER REYNOLDS-ZAHLEN MIT EINEM ZWEI-GLEICHUNGS-TURBULENZ-MODELL

Zusammenfassung—Die Veröffentlichung bringt numerische Berechnungen über verschiedene turbulente Strömungen, in denen die Struktur der viskosen Unterschicht beträchtlichen Einfluss auf die Strömung ausübt. Im zugrundegelegten Turbulenzmodell wird die Turbulenzenergie und deren Dissipationsanteil über die Transportgleichungen berechnet und zusammen mit den Erhaltungsgleichungen für die Hauptströmung gelöst. Die betrachteten Strömungen umfassen isotherme Rohrströmungen mit niedrigen Reynolds-Zahlen und Wandgrenzschichten mit Druckgradienten in Strömungsrichtung und Wandeinspritzung; die Voraussagen umspannen natürlichen Übergang und Laminarisation.

Obwohl vollständige Übereinstimmung mit dem Experiment noch nicht in jedem Fall erreicht ist, wird dargelegt, dass nur ein Turbulenzmodell von (mindestens) diesem Verwicklungsniveau ein allgemeines Erfassen der Turbulenzstrukturen nahe der Wand, wie sie gewöhnlich bei thermischen Problemen auftreten, erlaubt.

РАСЧЁТ ПРОЦЕССОВ ПЕРЕНОСА ПРИ НИЗКИХ ЗНАЧЕНИЯХ ЧИСЛА РЕЙНОЛЬДСА НА ОСНОВЕ МОДЕЛИ ТУРБУЛЕНТНОСТИ, СОСТОЯЩЕЙ ИЗ ДВУХ УРАВНЕНИЙ

Аннотация—В работе представлены численные решения для различных сдвиговых турбулентных течений, в которых структура вязкого подслоя оказывает существенное влияние на течение. В качестве модели турьулентности принимается модель, для которой энергия турбулентного движения и скорость её диссипации рассчитываются на основе соответствующих уравнений переноса, которые решаются совместно с уравнениями для осредненного течения.

Были исследованы изотермические течения в трубах при низких числах Рейнольдса и в пограничных слоях с положите льным градиентом давления на проницаемой стенке. Рассчитывался как переход, так и ламинаризация. Хотя еще не в каждом случае достигнуто полное соответствие с экспериментом, однако доказано, что только модель турбулентности такой сложности позволит универсальное моделирование структуры пристенных турбулентных течений, обычно обнаруживаемых в теплоэнергетических установках.